FLAMMABILITY OF POLYMER-CLAY NANOCOMPOSITES

by

Alexander B. Morgan, Jeffrey W. Gilman,
Takashi Kashiwagi and Catheryn L. Jackson
Building and Fire Research Laboratory
National Institute of Standards and Technology
Gaithersburg, MD 20899 USA

Reprinted from Fire Safety Developments Emerging Needs, Product Developments, Non-Halogen FR's, Standards and Regulations. Proceedings. Fire Retardant Chemicals Association. March 12-15, 2000, Washington, DC, 25-39 pp, 2000.

NIST
National Institute of Standards and Technology
Technology Administration, U.S. Department of Commerce

Flammability of Polymer-Clay Nanocomposites*

ABSTRACT

The flammability of two polymer-clay nanocomposites, made from polycaprolactam (PA-6) and polyethylene-co-vinylacetate (EVA) were investigated. Polymer-clay nanocomposites have the unique advantage of not only reducing the flammability of a polymer, but also improving the mechanical properties of the polymer. This is a key advantage over many flame retardants which improve flammability but reduce polymer mechanical properties. In our efforts to further understand the mechanism of flame retardancy with polymer-clay nanocomposites, we investigated the effects that clay dispersion and charring polymer additives might have on the flammability of the nanocomposite. The nanocomposites were analyzed by X-ray diffraction (XRD) and transmission electron microscopy (TEM) to determine the nature of the clay dispersion in the polymer. Cone calorimetry was used to evaluate the flammability of these nanocomposites. We determined that the type of dispersion of clay in the polymer (*intercalated* vs. *delaminated*) did not appear to have a major effect on flammability. Further, it appeared that the charring co-additive put in the PA-6 nanocomposites had no beneficial effect.

INTRODUCTION

Polymer-clay nanocomposites have attracted a great deal of interest due to their improved mechanical, thermal, and flammability properties.[1] More recent work in the Fire Science Division of the National Institute of Standards and Technology (NIST) has shown that polymer-clay nanocomposites exhibit reduced flammability and improved physical properties at low cost.[2] A wide variety of polymer resins have been used to synthesize polymer-clay nanocomposites via addition of an organically treated clay to a polymerization reaction (*in situ* method),[1b,3] to a solvent-swollen polymer (solution blending),[4] or to a polymer melt (melt blending).[1a,5] Our recent work, in concert with a recently formed flammability of polymer-clay nanocomposites consortium, has investigated nanocomposites made with two commodity polymers, namely polycaprolactam (PA-6) and polyethylene-co-vinylacetate (EVA), using melt blending. The PA-6 and EVA nanocomposites were montmorillonite (MMT) clay nanocomposites, where the sodium cations on the MMT had been replaced with organic ammonium salts. These organic ammonium salts served as the "treatment" for the clay, thus allowing the polymer to "wet" the surface of the clay and disperse the clay into the polymer.

The focus of our research on these two polymer-clay nanocomposites was to develop a fundamental understanding of the fire retardant (FR) mechanism provided by the clay. In that

* Alexander B. Morgan,[1] Jeffrey W. Gilman,[1] Takashi Kashiwagi[1], Catheryn L. Jackson[2]

[1] Fire Science Division, Building and Fire Research Laboratory,

[2] Polymer Division, Materials Science and Engineering Laboratory,

National Institute of Standards and Technology[†], Gaithersburg, MD 20899

attempt, we focused on comparing the flammability properties of: 1) *intercalated* versus *delaminated* nanocomposites, 2) nanocomposites with different silicate loading levels, and 3) nanocomposites incorporating a charring-resin, polyphenyleneoxide (PPO), into a blend.

POLYMER-CLAY NANOCOMPOSITE ANALYSIS

Each of the nanocomposite systems prepared was characterized using X-ray diffraction (XRD), and Transmission Electron Microscopy (TEM). XRD data was collected at ambient temperatures using CuK radiation with a 0.02 2q step size and a 2 s count time. Cone Calorimeter experiments were performed at an incident heat flux of 50 kW/m^2 using the cone heater[6]. Peak heat release rate (HRR), mass loss rate (MLR), specific heat of combustion (H_c), specific extinction area (SEA, a measure of smoke density), ignition time (t_{ign}), carbon monoxide yield, carbon dioxide yield, and specific heat of combustion data are reproducible to within ± a fraction of 10 % when measured at 50 kW/m^2 flux. The Cone data reported here are the average of three replicated experiments. The standard uncertainties (one sigma) are shown as error bars on the plots of the Cone data. Gasification experiments were performed using the gasification device built at NIST (Figure 1). The cylindrical chamber is 0.61 m in diameter and 1.70 m in height. Two windows provide optical access. The chamber walls are water cooled to 25 °C, and their interior surfaces are painted flat black. Products and ambient gases are removed via an exhaust duct, and a constant nitrogen flow of 7.67 L/s at 25 °C is maintained during the experiments. The temperature of the elements in the cone-shaped heater is fixed at 808 °C to maintain a constant emission spectrum for all tests. A water-cooled shutter was extended to protect the sample from the incident radiant flux during nitrogen purge, prior to testing. Flux levels varied about 8 % to10 % across the 0.1 m diameter sample region. The sample, 75 mm in diameter and 8 mm in thickness, was placed in an aluminum foil pan having nearly the same diameter as that of the sample, and 13 mm high side walls. The sample mass was measured by a load cell; these data were recorded at 0.5 s intervals. The Gasification device allows pyrolysis, in a nitrogen atmosphere, of samples identical to those used in the Cone Calorimeter, without complications from gas phase combustion, such as heat feedback and obscuration of the sample surface from the flame. The standard uncertainty in the measurement of interest in the gasification data is shown in each plot as an error bar.

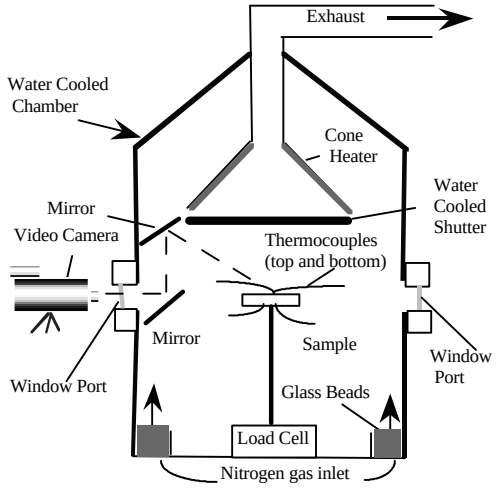

Figure 1. Schematic of Gasification device.

RESULTS AND DISCUSSION

PA-6 Nanocomposites: Characterization.

For the PA-6 nanocomposites, we looked at the effect of: (1) *intercalated* versus *delaminated* nanocomposites, (2) nanocomposites with different silicate loading levels and (3) nanocomposites incorporating a charring-resin, polyphenyleneoxide (PPO) into the blend, on the flammability of the nanocomposite. The nanocomposites were prepared to give an *intercalated* nanomorphology by extruding the PA-6 with dimethyl, dihydrogenated-tallow ammonium treated montmorillonite. XRD analysis showed the layer spacing to be 2.45 nm. TEM (Figure 2) shows tactoids with expanded interlayer spacings (d-spacings, or distance between clay layers) and confirms the intercalated structure. *Delaminated* PA-6 nanocomposites were prepared via the *in situ* method. Specifically, PA-6 was polymerized in the presence of the clay to give a *delaminated* nanocomposite. TEM (Figure 3) shows a *delaminated* PA-6/MMT nanocomposite. XRD of this material showed no peak, which is expected for a *delaminated nanocomposite*.[3b]

Figure 2. TEM of PA-6/5 % MMT showing the dispersed intercalated tactoids (dark lines). Scale for this image is 23.2 mm = 1 micron (1.0 μm)

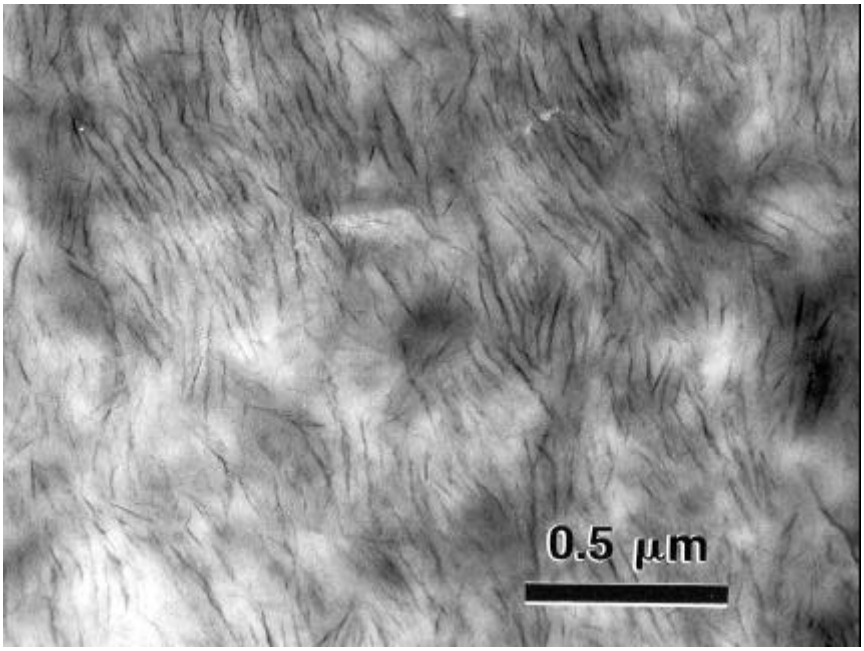

Figure 3. TEM of PA-6/5 % MMT showing the dispersion of *delaminated* clay layers (dark lines).

PA-6 Nanocomposites: Flammability.

The comparison of the heat release rate (HRR) behavior of the *intercalated* and the *delaminated* PA-6 nanocomposite is shown in Figure 4. The HRR curves are not significantly different. This indicates that *intercalated* and *delaminated* nano-morphologies are equally effective at reducing the flammability (HRR) of PA-6 nanocomposites made using MMT. However, a statistically significant difference in ignition times (t_{ign}) is evident between the *intercalated* and *delaminated* nanomorphologies from the HRR data in Figure 4. Specifically, the *intercalated* sample had a t_{ign} of 40 s compared to the t_{ign} of 80 s for the delaminated sample. The t_{ign} of the delaminated sample is similar to that for the pure PA-6 (t_{ign} 70 s). This shorter t_{ign} may be due to some physical effect (thermal conductivity, radiation absorption) or a chemical effect (thermal stability, volatile organic treatment).[7] In terms of possible chemical effects both the different methods of preparing the nanocomposites and the different MMT treatments may contribute to the earlier t_{ign}. The *delaminated* PA-6 nanocomposite sample is made via the *in situ* polymerization method, which uses an amino acid MMT treatment that becomes covalently bonded to the PA-6 as an end-group during the polymerization. The *intercalated* PA-6 nanocomposite, prepared via melt blending at 246 °C, with a quaternary alkyl ammonium treated MMT, does not bond the MMT treatment to the polymer. This may reduce t_{ign}, since the decomposition temperature of the quaternary alkyl ammonium treated MMT (200 °C) is 100 °C lower than that for the delaminated PA-6 nanocomposite.[2a] An additional effect may be due to processing. The melt blending process temperature (246 °C), used to make the intercalated PA-6 nanocomposite, is above the decomposition temperature of the quaternary alkyl ammonium treated MMT. Therefore decomposition products generated during processing may supply volatile fuel early in the Cone experiment and shorten t_{ign}.

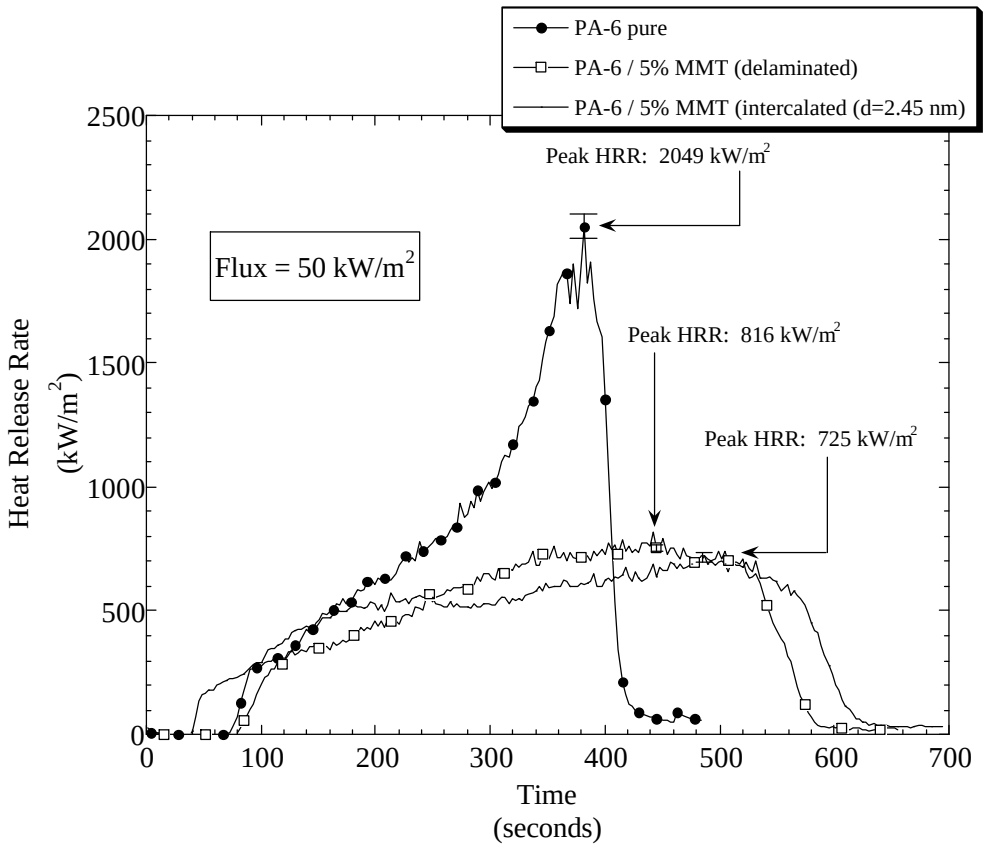

Figure 4. Heat release rate (HRR) data for pure PA-6, and intercalated and delaminated PA-6/MMT (mass fraction 5%) nanocomposites.

The effect of varying the MMT loading in PA-6 nanocomposites on the HRR is shown in Figure 5. The reduction in peak HRR improves as the mass fraction of MMT increases. The additional improvement for the PA-6/MMT nanocomposite with a MMT mass fraction 10 % is somewhat unusual, as we have observed with other polymer-clay nanocomposites that there is little improvement above the 5 % loading level.

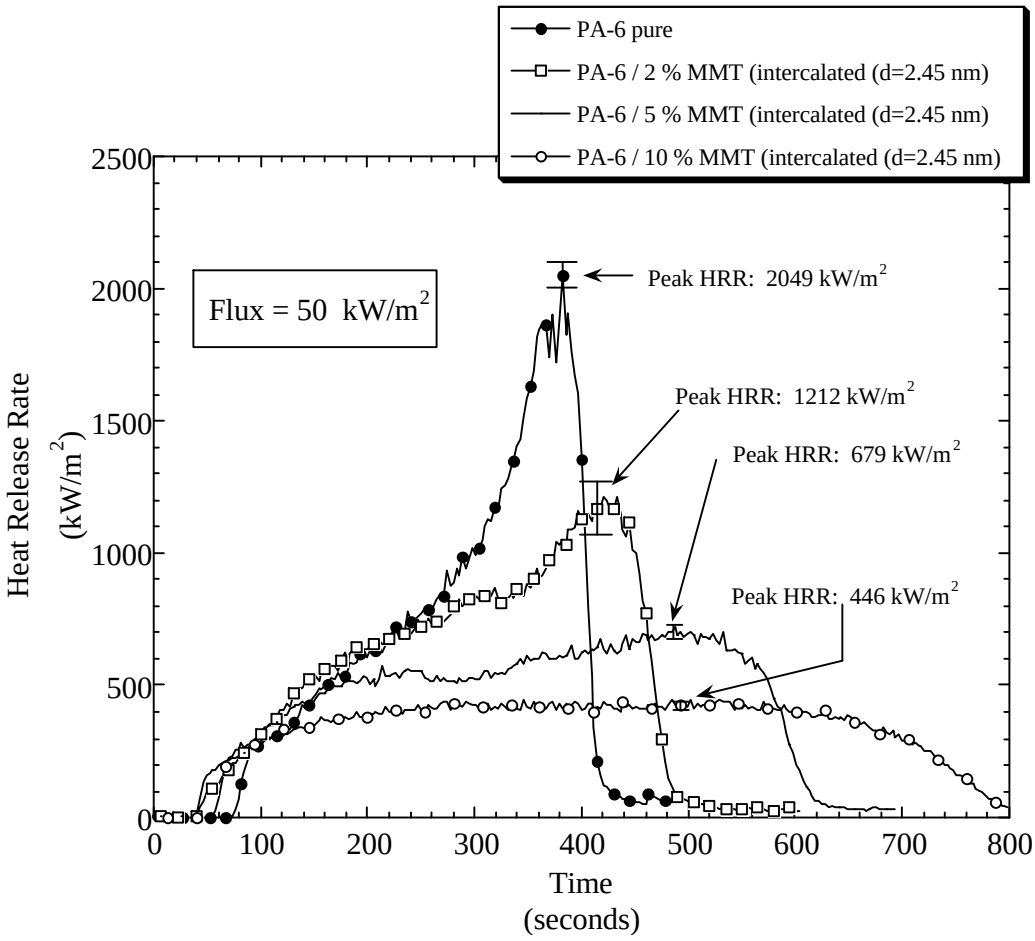

Figure 5. Heat release rate (HRR) data for pure PA-6, and intercalated PA-6/MMT nanocomposites (mass fractions 2 %, 5 % and 10 %).

In our initial studies on the flammability of PA-6 nanocomposites we found that a layered-silicate carbonaceous residue formed during combustion.[2a] However, there was very little additional carbonaceous char formed. We felt the use of an additive that would introduce additional carbonaceous char might enhance the effectiveness of the nanocomposite. To this end, PA-6 and polyphenyleneoxide (PPO) were extruded with the organic modified MMT. The HRR properties of these PA-6/PPO/MMT nanocomposites are shown in Figure 6.

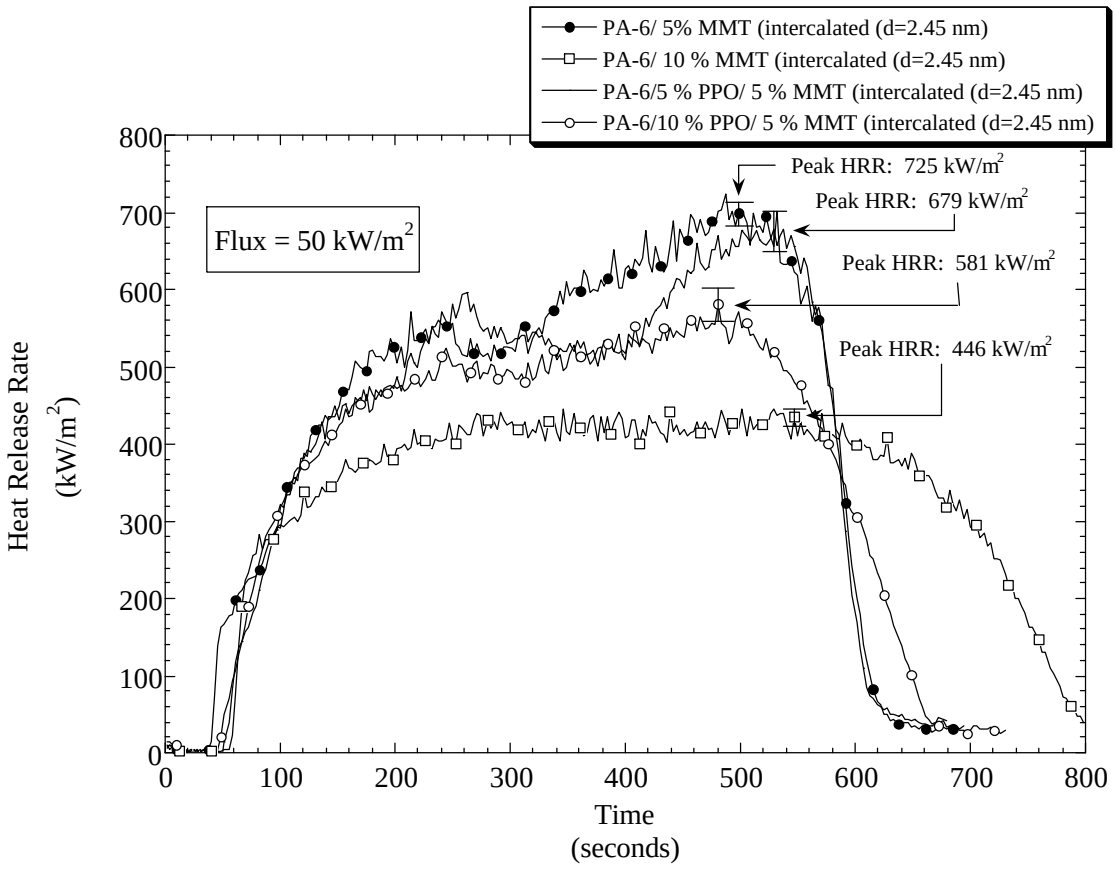

Figure 6. The HRR plots for PA-6/5 % MMT, PA-6/10 % MMT, PA-6/5 % PPO/5 % MMT and PA-6/10 % PPO/5 % MMT nanocomposites. All samples have intercalated nano-morphologies.

The introduction of PPO into the PA-6/MMT nanocomposites gives no improvement in HRR when added at the 5 % level. When 10 % PPO is added the HRR is lowered significantly. However this is in part due to the inherent lower HRR of PPO versus PA-6. The data in Figure 6 shows that the PA-6/10 % MMT actually out performs even the PA-6/10 % PPO/5 % MMT. The char yield of PPO is 40 %; possibly, use of another polymer that has a higher char yield is necessary to see the effect we envisioned.

In addition to measuring HRR the Cone Calorimeter also measures other fire-relevant properties such as MLR, H_c, SEA, carbon monoxide yield, and carbon dioxide yield. The HRR and the MLR data for the PA-6 nanocomposites discussed are the only parameters affected by the presence of nano-dispersed MMT in PA-6. The MLR data follows the loss of fuel from the condensed phase into the gas phase. In this case the MLR follows the volatilization of PA-6 decomposition products (primarily caprolactam). Figure 7 shows the MLR data for the intercalated and delaminated PA-6/MMT (mass fraction 5 %) nanocomposites.

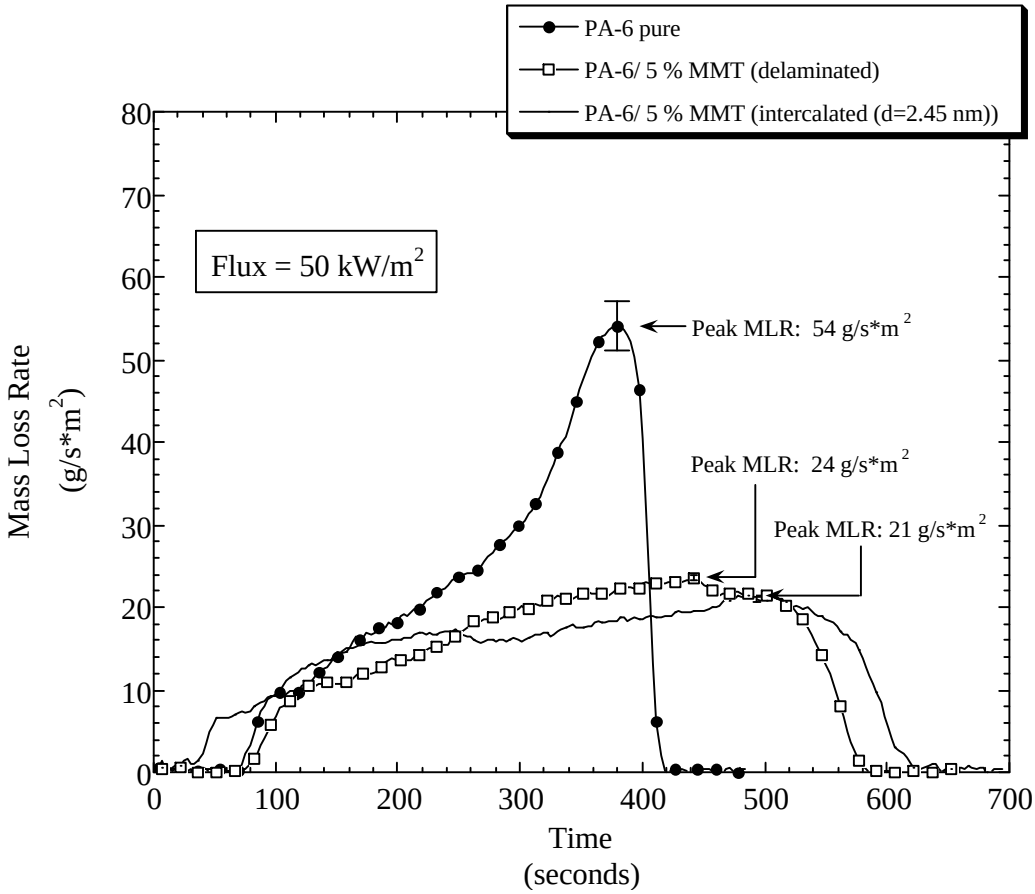

Figure 7. MLR data for PA-6 pure, intercalated and delaminated PA-6/MMT (mass fraction 5%) nanocomposites.

Comparison of Figure 4 to Figure 7, and recalling that none of the other parameters measured in the Cone were affected by the presence of nano-dispersed MMT, reveals that the nano-dispersed MMT reduces the HRR by reducing the MLR (fuel feed rate) of the nanocomposite. This is consistent with the results we found in our initial studies of the delaminated PA-6/MMT.[2a]

PA-6 Nanocomposites: Gasification.

As mentioned previously, the Gasification device allows pyrolysis, in a nitrogen atmosphere, of samples identical to those used in the Cone Calorimeter. Typically we measure MLR, and a video is taken of the sample inside the apparatus during the gasification. We evaluated the above series of PA-6/MMT nanocomposites using the Gasification apparatus and found that the MLR data showed the same trends as observed in the Cone experiments. Furthermore, we observed, from the video data, that a black-residue formed on the sample surface at about 150 s into the gasification experiment. The formation of this residue coincided with the reduced MLR. An additional observation we made is that the mass loss initiates earlier for all the PA-6/MMT nanocomposites as compared to the pure PA-6.

This is analogous to the observed shorter t_{ign} for all the PA-6/MMT nanocomposites found in the Cone data.

EVA nanocomposites: Characterization.

For the EVA nanocomposites, we looked at the effect of different silicate loading levels and organic treatments on the MMT. The nanocomposites were prepared with an *intercalated* nanomorphology by extruding the ethylene vinyl acetate copolymer (EVA, 18 % vinyl acetate) with several organic treated MMTs: a quaternary alkyl ammonium treated MMT (R4N), an octadecyl ammonium (ODA) treated MMT, and a dodecyl pyrrolidone (DDP) treated MMT. This allowed comparison of clay treatments in terms of their effectiveness in delaminating the clays. Both XRD and TEM were used to characterize the nano-morphology of the EVA/MMT nanocomposites. TEM indicates that the EVA sample containing the ODA treated MMT had good dispersion of the MMT throughout the sample, but with some intact intercalated-tactoids. XRD showed the d-spacing of these intercalated-tactoids to be 3.4 nm.

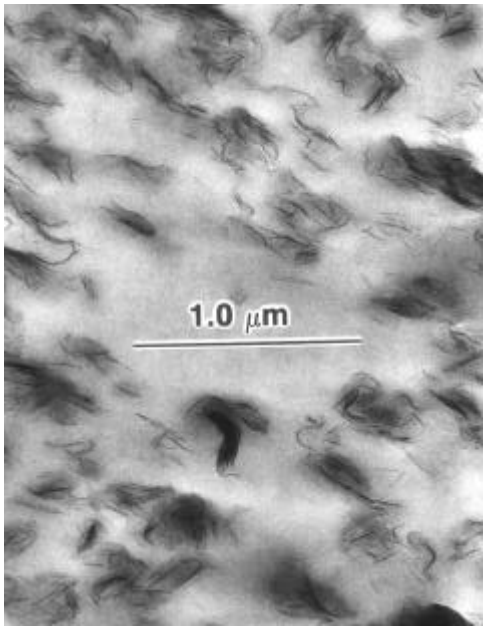

Figure 8. TEM of EVA/5 % MMT (ODA-MMT) showing typical intercalated /delaminated nano-morphology.

The EVA sample containing DDP treated MMT was not a uniform sample. It appears by TEM that the DDP treated MMT is immiscible in the polymer. Individual clay layers, even in large clay particles, were very hard to see even at high magnification. Further, this sample was not very stable in the presence of the electron beam, and decomposition of the sample occurred during observation with TEM. The XRD of these samples showed a smaller d-spacing (1.24 nm) after extrusion than before, i.e., they appeared to de-*intercalate* (see Table 1). The volatilization of DDP (b.p. of DDP is 200 °C) during extrusion (melt temperatures: 215 °C to 235 °C) would explain this result.

Table 1. Nano-morphology of EVA/MMT nanocomposites from XRD and TEM.

Sample	Actual Clay Loading [%]	Initial Clay d-spacing[a] [nm]	Final Composite d-spacing [nm][a]	Nano-morphology
EVA/2 % MMT (R4N)	2.1	2.24	3.64	Intercalated/ delaminated
EVA/5 % MMT (R4N)	6.7	2.24	3.43	Intercalated/ delaminated
EVA/10 % MMT (R4N)	9.7	2.24	3.44	Intercalated/ delaminated
EVA/5 % MMT (ODA)	2.2	2.18	3.42	Intercalated/ delaminated
EVA/2 % MMT (ODA)	6.4	2.18	3.43	Intercalated/ delaminated
EVA/5 % MMT(DDP)	2.1	4.21; 1.46*	1.24	-
EVA/2 % MMT(DDP)	5.3	4.21; 1.46*	1.24	-

* Two d-spacings were observed, one for the DDP treated MMT (4.21 nm) and one for MMT that had no DDP treatment (1.46 nm). The DDP clay can best be described as a clay containing two types of clay, one treated and the other untreated.

[a] d-spacings indicated here are the maximum point selected from a broader peak observed during the collection of the XRD data. The exact point is based on the real number (an actual data point) observed with the 0.02 2q step size having the largest intensity and appearing in the median of this broad peak.

EVA nanocomposites: Flammability.

The HRR data for the three EVA/5 % MMT samples are shown in Figure 9. The intercalated/delaminated EVA nanocomposites, EVA/5 % MMT (R4N) and EVA/5 % MMT (ODA), behave identically in the Cone; the reduction in HRR for both, compared to the HRR for pure EVA, is 69 %. Interestingly, EVA/5 % MMT (DDP) does show some reduction in HRR. Previously, in other polymer nanocomposite systems, we have shown that completely immiscible polymer-MMT composites have HRR that are unchanged from the pure polymer.[2] Therefore, the MMT in EVA/5 % MMT (DDP) may be partially nano-dispersed. The effect of varying the MMT loading on the HRR of the EVA/MMT nanocomposites is the same as that observed for other nanocomposites: the effect improves as the loading is increased from 2 % to 5 %, but no additional effect is seen for the 10 % samples. The initial HRR for the EVA/MMT samples is higher for the first minute following ignition. This effect is completely counteracted at 120 s into the experiment (80 s after ignition) by the formation of the MMT-reinforced carbonaceous-residue (char). The evidence that this char formation is responsible for the reduced HRR in the case of the intercalated/delaminated EVA nanocomposites, EVA/5 % MMT (R4N) and EVA/5 % MMT (ODA), comes from the gasification experiments.

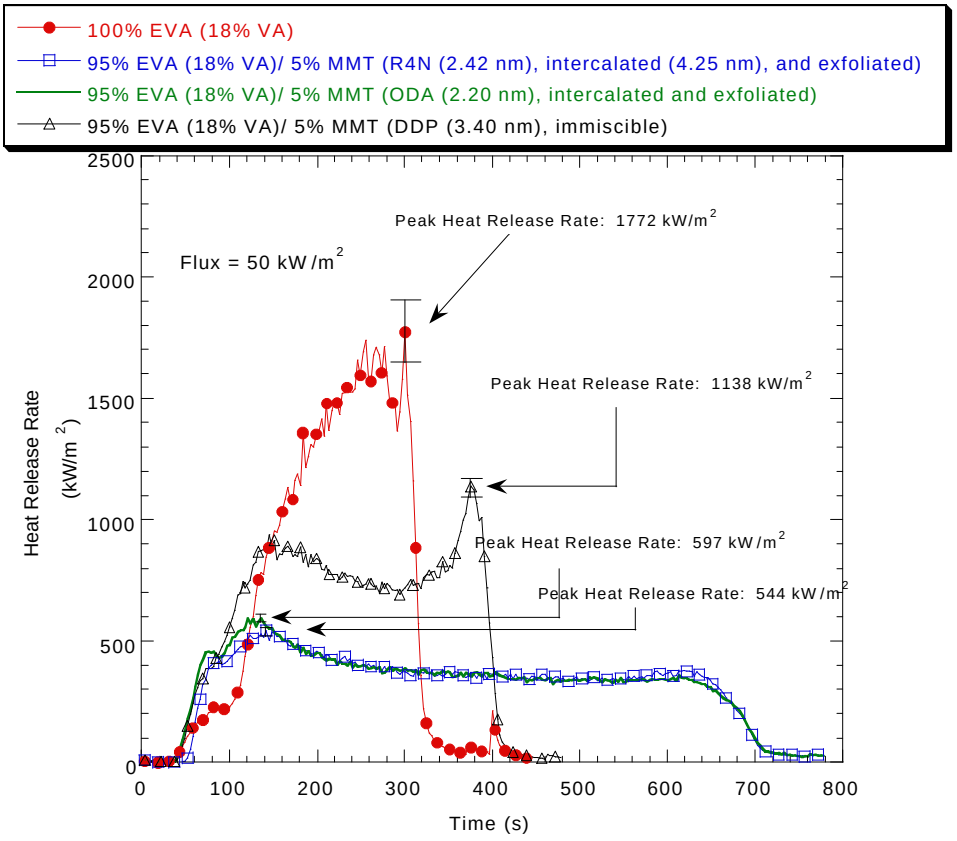

Figure 9. HRR plots for pure EVA, and the three EVA/5 % MMT samples each prepared with a different treated MMT.

EVA nanocomposites: Gasification.

Visual observation of the gasification experiments performed on the intercalated/delaminated EVA nanocomposites, EVA/5 % MMT (R4N) and EVA/5 % MMT (ODA) reveals that char formation begins within 60 s of the initial mass loss. The MLR data for the gasification experiments for the EVA/ MMT samples are shown in Figure 11. The same relative trends are observed in MLR as we found in HRR (Figure 11) for the three EVA/MMT samples. A striking difference is evident from examination of the digital photos of the residues from the gasification experiments of EVA/5 % MMT (R4N) and EVA/5 % MMT (DDP) shown in Figure 10. A continuous-monolithic carbonaceous-residue forms as a result of gasification of either, the EVA/5 % MMT (R4N) sample (shown below), or the EVA/5 % MMT (ODA) sample (not shown). However, the poorly dispersed EVA/5 % MMT (DDP) sample leaves only a light-gray residue which is essentially just MMT. Pure EVA gives a zero residue yield. Clearly, as we observed in the PS/MMT nanocomposites the otherwise non-char forming EVA is converted to a charring system by the nano-dispersed MMT.[2] Similar residues were formed from the Cone experiments.

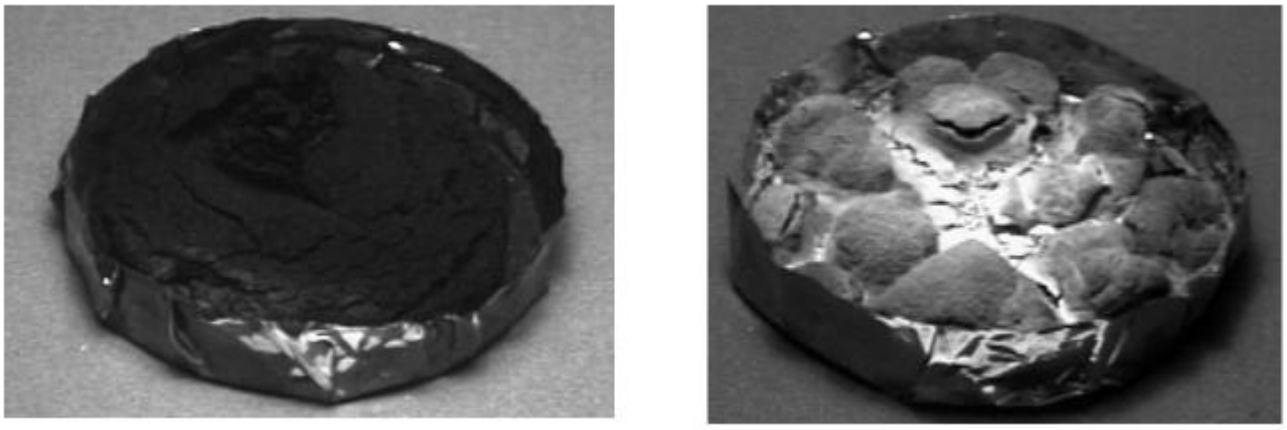

Figure 10. Digital photos of gasification residues from EVA/5 % MMT (R4N) (left) and EVA/5 % MMT (DDP) (right).

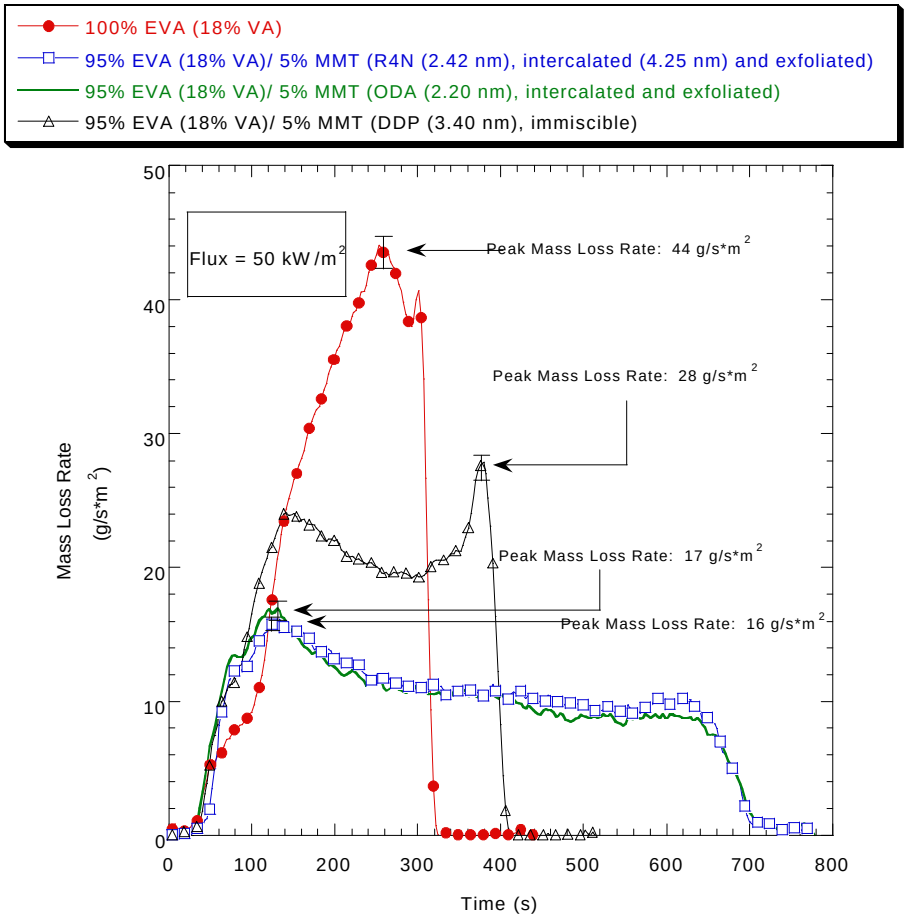

Figure 11. Mass Loss Rate data (flux: 50 kW/m^2) for pure EVA, and EVA/MMT samples with SCPX2156 (quaternary-MMT) or DDP (DDP-MMT) or ODA (ODA-MMT)

CONCLUSIONS

The most important result from our work on the flammability of polymer-clay nanocomposites is the formation of a clay-reinforced carbonaceous char during combustion of nanocomposites. This is particularly significant for systems whose base resin (PA-6, EVA) normally produces little or no char when burned alone. It appears from the gasification data (videos and mass loss data) that this clay-reinforced carbonaceous char is responsible for the reduced mass loss rates and hence the lower HRRs. Initially higher HRR and shorter t_{ign} are observed in many of the nanocomposites, and the origin of this effect needs to be better understood.

We conclude that *intercalated* PA-6 nanocomposites perform as well as *delaminated* PA-6 nanocomposites. In terms of the effect of loading level, the effectiveness of the nanocomposite approach to reducing HRR levels off at 5 % silicate loading for EVA and PA-6, although some additional effect for PA-6 is seen at 10 % clay loadings. And finally, the use of a char-enhancer (PPO) did not decrease the flammability of the PA-6 nanocomposites.

Unfortunately, while these PA-6 and EVA nanocomposites showed significantly lowered HRRs, they do not pass the UL-94 flammability test. Specifically, they did not obtain V-0, V-1, or V-2 ratings. However, several recent papers, patents, and patent applications show that the use of nano-dispersed clays (nanocomposites) in combination with other flame retardants do pass the UL-94 test (V-0). In most of these examples, the layered silicate nanocomposite replaces a certain amount of the flame retardant additive, allowing for some improvement in mechanical properties over the FR formulation containing no clay. For an EVA system, a PA-6 MMT nanocomposite was used to replace some of the pentaerythritol and ammonium polyphosphate (APP) in a typical APP based intumescent flame retardant formulation.[8] As much as 1/3 of the APP could be removed while maintaining a UL-94 V-0 result, and the elongation of the resulting EVA FR material is increased from 800% to 850%. This replacement approach was also used with a polybutylene terephthalate (PBT) system.[9] In this system, an organically modified MMT was used in combination with polytetrafluoroethylene (PTFE) dispersed in a styrene-acrylonitrile (SAN) copolymer [50% PTFE] to replace 40 % of the brominated polycarbonate-Sb_2O_3 mixture needed to give UL-94 V-0 rating to the PBT blend. This replacement allowed the UL-94 V-0 rating to be maintained. There are other examples of layered-silicate nanocomposites (where the layered silicate is MMT or a synthetic material, such as fluorinated synthetic mica) used with conventional flame retardants such as decabromodiphenyl ether/Sb_2O_3 or melamine to obtain UL-94 V-0 results.[10]

In light of these results, polymer-clay nanocomposites become a powerful tool for the flame retardant chemist. It offers the chemist an additive which can reduce the flammability of a polymer with no detrimental effects on the mechanical properties of the polymer system.

ACKNOWLEDGMENTS[‡]

[‡] Certain commercial equipment, instruments, materials, services or companies are identified in this paper in order to specify adequately the experimental procedure. This in no way implies endorsement or recommendation by NIST.

We would like to thank the Flammability of Polymer-Clay Nanocomposites Consortium for funding of this work. We would also like to thank members of NIST-BFRL for their assistance in this research: Mr. Richard Harris, Jr., for injection molding and sample preparation, Mr. Michael Smith for Cone Calorimeter work, Ms. Lori Brassell for sample preparation and cone calorimeter data analysis, and Mr. John Shields for Gasification apparatus work. We would also like to thank Dr. James Cline of NIST-MSEL for use of the Ceramics Division XRD facilities. We would also like to acknowledge General Electric Inc. for the TEM image of the *intercalated* PA-6 nanocomposite (Figure 2).

REFERENCES

1 (a) Gianellis, E. P. *Advanced Materials* **1996**, *8*, 29. (b) Kojima, Y.; Usuki, A.; Kawasumi, M.; Okada, A.; Fukushima, Y.; Kurauchi, T.; Kamigaito, O. *J. Mater. Res.* **1993**, *8*, 1185. (c) Wang, Z.; Pinnavaia, T. J. *Chem. Mater.* **1998**, *10*, 1820. (d) Burnside, S. D.; Giannelis, E. P. *Chem. Mater.* **1995**, *7*, 1597. (e) Lee, J.; Takekoshi, T.; Giannelis, E. P. *Mat. Res. Soc. Symp. Proc.* **1997**, *457*, 513.

2 (a) Gilman, J. W.; Kashiwagi, T.; Lichtenhan, J. D. *SAMPE Journal* **1997**, *33*, 40. (b) Gilman, J. W.; Kashiwagi, T.; Brown, J. E. T.; Lomakin, S.; Giannelis, E. P.; Manias, E. *Proceedings of 43rd Inter. SAMPE Symp. And Exib.* **1998**, 1053. (c) Gilman, J. W.; Kashiwagi, T.; Nyden, M.; Brown, J. E. T.; Jackson, C. L.; Lomakin, S.; Giannelis, E. P.; Manias, E. Chemistry and Technology of Polymer Additives. The Royal Society of Chemistry, Cambridge, 1999, 249-265. (d) Gilman, J. W. *App. Clay Sci.* **1999**, *15*, 31.

3 (a) Fujiwara, S.; Sakamoto, T. *Kokai Patent Application*, no. SHO 51(1976)-109998 (1976). (b) Lan, T.; Pinnavaia, T. J. *Chem. Mater.* **1994**, *6*, 2216. (c) Usuki, A.; Kato, M.; Okada, A.; Kurauchi, T. *J. App. Polym. Sci.* **1997**, *63*, 137. (d) Meier, L. P., Shelden, R. A.; Caseri, W. R.; Suter, U. W. *Macromolecules* **1994**, *27*, 1637. (e) Reichert, P.; Kressler, J.; Thomann, R.; Mulhaupt, R.; Stoppelmann, G. *Acta Polymer.* **1998**, *49*, 116.

4 Jeon, H. G.; Jung, H. T.; Less, S. D.; Hudson, S. *Polymer Bulletin* **1998**, *41*, 107.

5 (a) Maxfield, M.; Christiani, B. R.; Murthy, S. N. ; Tuller, H. US Patent 5,385,776 (1995). (b) Fisher, H.; Gielgens, L.; Koster, T. Nanocomposites from Polymers and Layered Minerals: TNO-TPD Report (1998).

6 Babrauskas, V., Fire and Materials, **1995**, 19, 243.

7 The Cone data for pure PA-6 shown in the HRR and MLR plots is for the material from UBE. However the PA-6 used by GE to prepare the nanocomposites (from Allied Signal) has very similar flammability properties to the UBE material.

8 Bourbigot, S.; Le Bras, M.; Dabrowski, F.; Gilman, J. W.; Kashiwagi, T. *Fire and Materials*, submitted for publication.

9 Takekoshi, T.; Fouad, F.; Mercx, F. P. M.; De Moor, J. J. M. US Patent 5,773,502 – issued to General Electric Company, 1998.

10 (a) Inoue, H.; Hosakawa, T. *Japan Patent Application* (Showa Denko K. K., Japan) Jpn. Kokai tokkyo koho JP 10 81,510 (98 81,510) (1998). (b) Okada, K. (Sekisui) *Japan Patent* 11-228748, (1999).